

Versatility and dynamics of the copper(I) coordination sphere in sterically hindering tris(pyrazolyl)methane-incorporating macrobicycles†‡

Leyong Wang,^{ab} Jean-Claude Chambron^{*a} and Enrique Espinosa^{ac}

Received (in Montpellier, France) 22nd September 2008, Accepted 28th November 2008

First published as an Advance Article on the web 8th January 2009

DOI: 10.1039/b816275a

Two arene-capped macrobicycles (**1** and **2**) incorporating the tris(pyrazolyl)methane (Tpm) chelate have been prepared from a benzylthiol-functionalized Tpm precursor (**3**). Reaction of either macrobicycles with $\text{Cu}(\text{CH}_3\text{CN})_4^+$ leads to tetrahedral or trigonal-planar, fluxional complexes incorporating the $\text{Cu}(\text{CH}_3\text{CN})^+$ subunit ($[\text{Cu}(\mathbf{1})(\text{CH}_3\text{CN})]^+$ and $[\text{Cu}(\mathbf{2})(\text{CH}_3\text{CN})]^+$). The acetonitrile ancillary ligand does not fit inside the macrobicycles cavity and can be removed by heating under vacuum, which produces the $[\text{Cu}(\mathbf{1})]^+$ and $[\text{Cu}(\mathbf{2})]^+$ species probably involving intramolecular thioether coordination. The $[\text{Cu}(\mathbf{1})(\text{CH}_3\text{CN})]^+$ complex was shown to convert slowly in wet acetone into a helical coordination polymer, which is formulated as $[\text{Cu}(\mathbf{1})(\text{H}_2\text{O})]_n^{n+}$. In the crystal, the metal cation in tetrahedral geometry is bound to two pyrazole nitrogens and bridges two macrobicyclic subunits by intermolecular thioether sulfur coordination. Its coordination sphere is remarkably completed by a water molecule that is located inside the macrobicycles and is bound to the uncoordinated pyrazole fragment and to the mesitylene cap by $\text{OH} \cdots \text{N}$ and $\text{OH} \cdots \pi$ hydrogen bonding interactions.

Introduction

The stereoelectronic control of the coordination sphere of transition metal cations by multidentate ligands is an important issue in the design of mimics of the active sites of metallo-enzymes and the development of homogeneous catalysts. Ligands that favor coordinatively unsaturated transition metal complexes and enforce unusual coordination numbers are particularly relevant in this context, as these systems are often particularly reactive.¹ As a matter of fact, the activation of otherwise inert molecules, such as dinitrogen, has amply relied on these principles.²

Sterically encumbering ligands can be designed by grafting bulky substituents in close proximity to the coordinating sites,³ or by incorporating the latter in macro(poly)cyclic structures,⁴

these approaches being inspired by the concept of enzyme pockets, and producing confined environments such as those offered by metal-modified zeolites,⁵ or self-assembled cages.⁶

Multiple examples of sterically encumbered ligands can be found in the scorpionate family, especially the anionic tris(pyrazolyl)hydroborates ($\text{Tp}^{\text{R},\text{R}'}$).⁷ Substitution of the pyrazole 3-position (R') by sterically hindering groups enforces tetrahedral coordination geometry at the metal and allows control of the fourth, apical coordination site. For example, four-coordinate monomeric Cu(II) thiolato complexes, that bear spectroscopic similarities to blue copper proteins, have been obtained with the $\text{Tp}^{\text{Pr},\text{Pr}}$ ligand.⁸ The use of bulky, hydrophobic substituents such as *t*-butyl in $\text{Tp}^{\text{Bu},\text{Me}}$ has led to the discovery of a Zn(II) complex that is a structural and functional mimic of carbonic anhydrase.⁹ The Cu(I) complex of *trans*- Tp^{pm} , a tris(pyrazolyl)hydroborate ligand featuring a deep, C_3 -symmetric chiral cavity, gave 85% ee for the *cis* product of the catalytic enantioselective cyclopropanation of styrene by ethyl diazoacetate.¹⁰

A few metal complexes with sterically hindered tris(pyrazolyl)methane (Tpm) analogues of the Tp ligands have been reported. Silver(I) forms complexes of 1 : 1 stoichiometry only in the presence of the bulky Tpm^{Bu} ligand,¹¹ but cationic tetrahedral copper(I) carbonyl and acetonitrile complexes with Tpm^{Ph} or Tpm^{Bu} do not differ from those with $\text{Tpm}^{\text{Me},\text{Me}}$.¹²

We recently communicated on the synthesis of macrobicycles **1** that incorporates the tris(pyrazolyl)methane chelate (Scheme 1).¹³ As suggested by handling of Corey–Pauling–Koltun molecular models, the cavity left over copper(I) coordinated to the three pyrazole nitrogens is not large enough to accommodate a small, rigid rod axial ligand such as CH_3CN . We were therefore intrigued to know how this metal, which shows preference for tetrahedral coordination geometry in normal conditions, but turns to trigonal-planar (or even

^a Institut de Chimie Moléculaire de l'Université de Bourgogne (ICMUB, UMR CNRS n° 5260), 9 avenue Alain Savary, BP 47870, 21078 Dijon cedex, France

E-mail: jean-claude.chambron@u-bourgogne.fr;

Fax: +33 (0)3 8039 6117; Tel: +33 (0)3 8039 6116

^b Key Laboratory of Mesoscopic Chemistry of Ministry of Education and School of Chemistry and Chemical Engineering, Nanjing University, 210093 Nanjing, P.R. China. E-mail: lywang@nju.edu.cn

^c Laboratoire de Cristallographie et Modélisation des Matériaux Minéraux et Biologiques (LCM3B, UMR CNRS n° 7036), Nancy-Université, 1 boulevard des Aiguillettes,

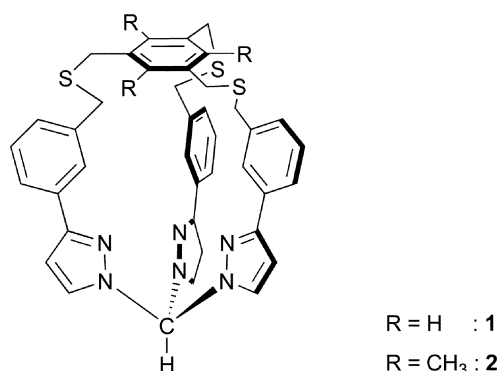
54606 Vandœuvre-lès-Nancy, France.

E-mail: enrique.espinosa@lcm3b.uhp-nancy.fr;

Fax: +33 (0)3 8340 6492; Tel: +33 (0)3 8368 4953

† Dedicated to Prof. Jean-Pierre Sauvage on the occasion of his 65th birthday.

‡ Electronic supplementary information (ESI) available: Synthesis of compound **3** and its precursors; NOESY 2D $^1\text{H}/^1\text{H}$ NMR spectra of **1** and $[\text{Cu}(\mathbf{1})(\text{CH}_3\text{CN})]\text{PF}_6$, VT ^1H NMR spectra of **1**, $[\text{Cu}(\mathbf{1})(\text{CH}_3\text{CN})]\text{PF}_6$, $[\text{Cu}(\mathbf{2})(\text{CH}_3\text{CN})]\text{PF}_6$, $[\text{Cu}(\mathbf{1})]\text{PF}_6$, and $[\text{Cu}(\mathbf{2})]\text{PF}_6$; X-ray crystallographic data for **1** and $[\text{Cu}(\mathbf{1})(\text{H}_2\text{O})_n](\text{PF}_6)_n$. CCSC 710458–710459. For ESI and crystallographic data in CIF or other electronic format see DOI: 10.1039/b816275a



Scheme 1 Structural formulae of the macrobicycles.

linear) under steric pressure,¹⁴ would respond to the constraints imposed by the macrobicyclic ligand.

This report adds a new member to this family of sterically hindered scorpionate molecules, **2**, which derives from **1** by methyl substitution of the benzene cap, and examines their coordination chemistry with copper(I).

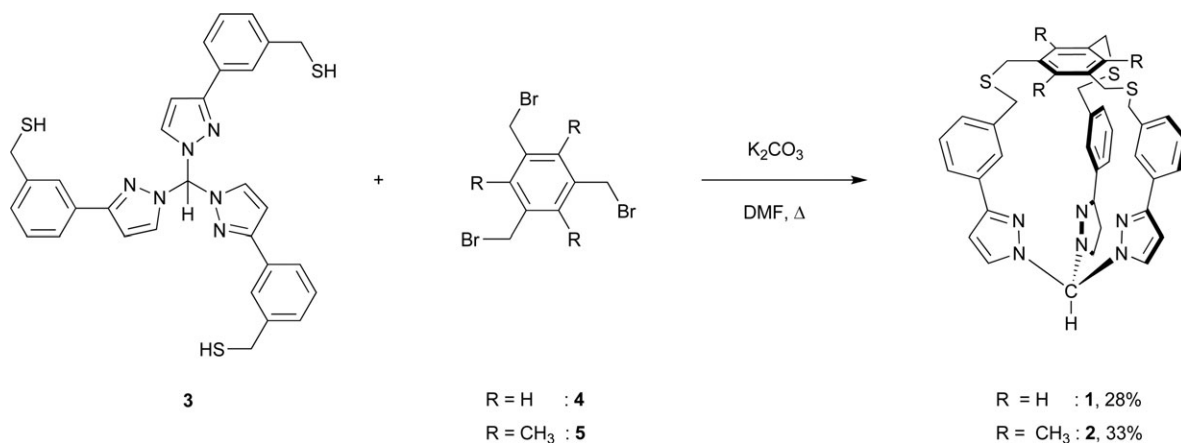
Results and discussion

Synthesis of the macrobicycles

Macrobicycles **1**¹³ and **2** were prepared by tripod–tripod coupling reaction between benzylthiol-functionalized tris(pyrazolyl)methane **3**¹³ and either 1,3,5-tribromomethylbenzene **4** or 1,3,5-tribromomethyl-2,4,6-trimethylbenzene **5**, in the presence of K₂CO₃ as base, in *N,N*-dimethylformamide (DMF) at 60 °C under high dilution (1.7 mM) (Scheme 2). In these conditions, they were obtained in 28%¹³ and 33% yields for **1** and **2**, respectively, after purification by column chromatography.

Structures of the macrobicycles

Comparison of the MALDI-TOF spectra of **1** and **2** with the spectrum of acyclic precursor **3** attests to the macrobicyclic nature of the former. Whereas for the closed structures **1** and **2** the highest *m/z* corresponds to the molecular peak (respectively, 694 and 738), in the case of the open system **3** it corresponds to a bis(pyrazolyl)methane fragment (*m/z* 391), the expected molecular peak at *m/z* 581 being not observed.



Scheme 2 Preparation of macrobicycles **1** and **2**.

This suggests that one C(methine)–N(pyrazole) bond is cleaved under laser irradiation. This fragmentation process presumably also happens in the case of the macrobicycles. However, since the released pyrazole-containing arm is still attached to the rest of the molecule, the observed signal corresponds to the molecular peak.

Macrobicycles **1** and **2** have similar ¹H NMR spectra (CDCl₃, CD₂Cl₂) and display C_{3v} symmetry in solution (Table 1). The spectrum of **1** was assigned using ¹H/¹H 2D NOESY, which shows the following through space correlations: 5'-H/CH, 4'-H/4-H, ArH/2-H, ArCH₂S/ArH, SCH₂/2-H, and SCH₂/6-H (Fig. S1, ESI†). The correlation ArH/2-H shows that the molecule has a dwarfed conformation obtained by squeezing the benzene cap towards the Tpm chelate. The methylene protons are enantiotopic, even at 190 K, where two close, although slightly broadened singlets are still observed (Fig. S2, ESI†). Comparison of **1** and **2** with precursor **3**, which has an open, acyclic structure indicates that methine protons are mostly affected by the conformational change ($\Delta\delta \approx -0.35$ ppm), whereas pyrazole protons 4'-H and 5'-H are not. Other protons that show significant shifts are 2-H and 4-H of the phenyl rings ($|\Delta\delta| \geq 0.2$ ppm for **2**). Their *ortho* position to the pyrazole subunit makes the former obviously sensitive to conformational changes about the pyrazole–phenyl bond. The methylene protons are also affected ($\Delta\delta \approx -0.22$ ppm).

Macrobicyclic **1** formed suitable X-ray quality crystals by slow evaporation of a dichloromethane–heptane solution, and its crystal structure was solved. Two non-equivalent molecules share the unit cell (Fig. 1): one encapsulates a water molecule, the other is empty. The two macrobicycles are perpendicular to each other, the *m*-phenylene spacer of the empty one showing π – π stacking interactions with the benzene cap of the other, with a 3.706 Å distance between centroids and a 2.2° angle between the mean planes of the aromatic fragments. The *m*-phenylene spacers of the empty molecule are nearly coplanar with the pyrazole subunits, the angles between their mean planes ranging from 14.2° to 19.7°. Two spacers of the other molecule are tilted to some extent, with angles of 32.1° and 33.7°. This is presumably the result of the encapsulation of a water molecule, which is equally disordered on two positions, one outside and the other inside the macrobicyclic.

Table 1 ^1H NMR data of tripod precursor **3**, macrobicycles **1** and **2**, and their copper(I) complexes^a

Solvent Compound ^b	CDCl_3			d_6 -acetone (CD_2Cl_2)			d_6 -acetone		
	1	2	3	1	$[\text{Cu}(\mathbf{1})\text{ACN}]^+$	CIS (1)	$[\text{Cu}(\mathbf{2})\text{ACN}]^+$	$[\text{Cu}(\mathbf{1})]^+ (\Delta\delta)^f$	$[\text{Cu}(\mathbf{2})]^+ (\Delta\delta)^g$
CH	8.13	8.17	8.50	9.02 (8.16)	9.41 ^{d,e} (8.82)	+0.39 (+0.66)	9.40	9.55 (+0.14)	9.39 (−0.01)
5'	7.66	7.73	7.68	8.04 (7.73)	8.44 (8.24)	+0.40 (+0.51)	8.45	8.46 (+0.02)	8.45 (0.00)
2	7.66	7.58	7.79	7.96 (7.68)	8.14 (8.05)	+0.18 (+0.37)	8.17	8.03 (−0.11)	8.06 (−0.11)
4	7.42	7.43	7.68	7.51 (7.45)	7.67 (7.61)	+0.16 (+0.16)	7.63	7.62 (−0.05)	7.60 (−0.03)
6	7.38	7.32	7.31	7.43 (7.42)	7.62 (7.51)	+0.19 (+0.09)	7.50	7.57 (−0.05)	7.45 (−0.05)
5	7.31	7.29	7.36	7.32 (7.34)	7.46 (7.43)	+0.14 (+0.09)	7.39	7.43 (−0.03)	7.35 (−0.04)
ArH	7.03			7.23 (7.08)	7.32 (7.19)	+0.09 (+0.11)		7.29 (−0.03)	
4'	6.63	6.64	6.69	6.70 (6.67)	6.99 (6.69)	+0.29 (+0.02)	7.01	6.97 (−0.02)	6.98 (−0.03)
ArCH ₂ S	3.62	3.73		3.81 (3.67)	3.92 (3.83)	+0.11 (+0.16)	4.09	3.90 (−0.02)	4.07 (−0.02)
CH ₂ S	3.60	3.52	3.78	3.73 (3.63)	3.85 (3.79)	+0.12 (+0.16)	3.91	3.75 (−0.10)	3.82 (−0.09)
ArCH ₃		2.04					2.45		2.42 (−0.03)
CH ₃ CN				2.05 (1.97) ^c	1.90 (1.66)	−0.15 (−0.31)	2.03		

^a Unless otherwise stated, the spectra were recorded at 500 MHz and 300 K. Chemical shifts are given in ppm downfield from SiMe_4 . ^b Numbering scheme as shown in Fig. 2. ^c Refers to free CH_3CN in d_6 -acetone (respectively, CD_2Cl_2). ^d 298 K. ^e 600 MHz. ^f $\Delta\delta$ (ppm) refers to the chemical shift difference between homologous protons of $[\text{Cu}(\mathbf{1})]^+$ and $[\text{Cu}(\mathbf{1})\text{ACN}]^+$. ^g Same as (f) for the complexes of **2**.

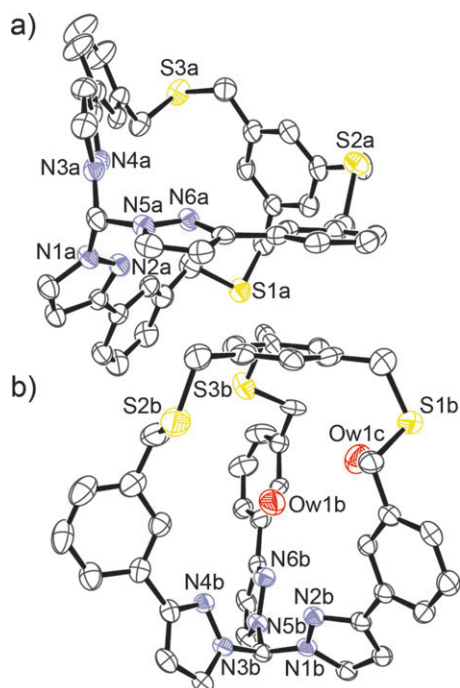


Fig. 1 ORTEP view of a pair of non-equivalent molecules in the crystal structure of **1**. The depicted H_2O solvate (shown in (b)) is disordered over two positions, one inside, the other outside the cavity. Ellipsoids are drawn at 50% probability level.

inside water molecule is well centered in the cavity of the cage, with very similar $\text{O}\cdots\text{N}$ bond distances that range from 3.297(6) Å to 3.447(6) Å, and a distance of 4.521 Å between the oxygen atom and the centroid of the mesitylene cap. The corresponding angles range from 141.1° to 156.1°. These data indicate that the inside water molecule forms hydrogen bonds with two pyrazole N atoms.

Macrocycles **1** and **2** have the unique property of incorporating a tris(pyrazolyl)methane scorpionate ligand in its conformation for making metal complexes with trigonal-pyramidal or tetrahedral geometry. The degree of preorganization

could be estimated by comparing relevant geometric parameters for the empty cage and related copper(I) tris-(pyrazolyl)methane complexes. For example, in the case of $[\text{Cu}(\text{Tpm}^{\text{tBu}})(\text{CH}_3\text{CN})]\text{PF}_6$,¹² $\text{N}\cdots\text{N}$ distances between coordinating atoms range from 2.925 to 2.987 Å, while they are slightly longer for **1** (2.915–3.514 Å). Other representative parameters, the angles between the vectors joining the methine carbon and the coordinating nitrogen atoms, are within the same limits for both compounds (Table S1, ESI†).

The complexation of Cu(I) by the macrobicycles

The coordination chemistry of macrobicycles **1** and **2** was investigated with copper(I), a prototypical metal cation that shows preference for trigonal-planar and tetrahedral coordination environments, depending on the number of available donor atoms.

Reaction of equimolar amounts of **1** and $[\text{Cu}(\text{CH}_3\text{CN})_4]\text{PF}_6$ in CH_2Cl_2 – CH_3CN 2 : 1 for 2 h, followed by evaporation of the solvents and drying under vacuum at 35 °C for 12 h left a material that was examined by ^1H and ^{13}C NMR. The colorless product of the reaction did not dissolve completely in CD_2Cl_2 , but was apparently more soluble in d_6 -acetone. § The mixtures were therefore clarified by filtration. The spectra of the resulting solutions differ from that of the free macrobicyclic ligand in the corresponding solvents, which indicates that complexation has indeed taken place. Complexation induced shifts (CIS) of macrobicyclic ligand **1** are all positive (Table 1). In CD_2Cl_2 , the highest CIS are observed for the methine CH (+0.66 ppm) and 5'-H (+0.51 ppm), while 4'-H shows the lowest (+0.02 ppm). 2-H is also affected significantly (+0.37 ppm), which suggests some reorientation of the *m*-phenylene spacers upon complexation, but methylene (+0.16 ppm), benzene (+0.11 ppm) and other aryl protons (+0.09 ppm) are, by comparison, only slightly shifted. In addition to the signals of the complexed macrobicyclic ligand a singlet at δ 1.66 ppm integrating for \approx 3 H is due to Cu(I)-bound CH_3CN . It is shielded by −0.31 ppm with respect to free CH_3CN (δ 1.97 ppm in CD_2Cl_2). All the peaks broaden upon decreasing the temperature,

§ This made the determination of yields difficult.

especially those of the aryl and methylene groups, with a maximum broadening of the macrobicyclic protons at 210 K, which is characteristic of coalescence (Fig. S3, ESI†). Below, smaller peaks separate from the main set of signals, while the methine CH, 4'-H and 5'-H of the latter sharpen again. This indicates that, at low temperature (182 K), the Cu(I) complex of **1** has a major conformation that is accompanied by minor one(s). The singlet of the CH₃CN protons broadens as the temperature is lowered, but its chemical shift does not change throughout. At least two very broad, overlapping peaks have separated in the 182 K spectrum. The spectral evolution is different in d₆-acetone, as simple monotonous broadening is observed upon cooling (Fig. S4, ESI†). At 182 K at least three broad signals are observed in the region of the methylene protons, which probably indicates that the latter form diastereotopic pairs below this temperature, their coalescence occurring at ≈190 K.

Except for 4'-H (+0.29 vs +0.02 ppm in CD₂Cl₂), the CIS values are all decreased in acetone, including the bound acetonitrile molecule (−0.15 vs −0.31 ppm in CD₂Cl₂). The nitrile carbon (δ 106.2) also resonates upfield by comparison with uncomplexed CH₃CN in d₆-acetone (δ 117.6 ppm). The ¹H/¹H NOESY 2D spectrum (Fig. S5, ESI†) shows the following correlations: 5'-H/CH, 4'-H/4-H, ArCH₂S/ArH, SCH₂/2-H, and SCH₂/6-H, which are indicated in Fig. 2. In addition to these features, there is a remarkable correlation spot between the protons of the bound CH₃CN and those of the benzene cap (ArH). All these observations allow formulation of the complex as [Cu(**1**)(CH₃CN)]⁺. The latter can be formed directly in d₆-acetone from **1** and Cu(CH₃CN)₄⁺. Only one singlet for the CH₃CN molecules (integrating for 12 protons) is observed at 2.02 ppm (vs 1.90 ppm in the case of pure [Cu(**1**)(CH₃CN)]⁺ dissolved in d₆-acetone), which indicates that the bound and free acetonitrile molecules are in fast exchange on the ¹H NMR timescale. Removal of the solvent under vacuum at 40 °C overnight left a colorless solid, which again did not completely dissolve in d₆-acetone, but analyzed as [Cu(**1**)(CH₃CN)]⁺, as shown by ¹H NMR spectroscopy.

By contrast, the Cu(I) complex of **2** prepared similarly dissolves easily in d₆-acetone. However, its ¹H NMR spectrum in this solvent shows broad features at 300 K, except for the CH₃CN protons. As increasing the temperature sharpens the signals, line broadening is diagnostic of dynamic effects in the complex (Fig. 3). Indeed, macrobicyclic **2** itself has sharp resonances at 300 K. As shown in Table 1, analogous protons of **1** and **2** in their complexes have similar δ, with the exception of protons 6-H and ArCH₂S, which are close to the mesityl cap, and show |Δδ| > 0.10 ppm. This is not surprising, as the macrobicyclics differ by the very nature of the cap. Similar features are found in the ¹H/¹H NOESY 2D spectrum of [Cu(**2**)(CH₃CN)]⁺, except that the correlation ArCH₂S/ArH of [Cu(**2**)(CH₃CN)]⁺ is replaced by correlations ArCH₂S/CH₃ and CH₂S/CH₃. However, the correlation CH₃/CH₃CN is notably absent.

The dynamic NMR features of the Cu(I) complex of **2** in d₆-acetone differ significantly from those of [Cu(**1**)(CH₃CN)]⁺. Contrary to the latter case, decreasing the temperature gradually sharpens the signals at first, with a maximum at 240 K (Fig. 3). Further cooling considerably broadens the signals of the 2-H and methylene protons, while the others just broaden a little. The signal of CH₃CN broadens monotonously between 300 and 182 K, and shifts downfield from 2.02 to 2.21 ppm (Fig. S6, ESI†).

At first glance macrobicyclic **1** forms a C_{3v} symmetric copper(I) complex at the ¹H NMR timescale, with a bound acetonitrile molecule. However, this ancillary ligand is not located inside the macrobicyclic, otherwise the resonance of the methyl protons would appear much more upfield. The data also rule out the direct interaction of copper(I) with the mesitylene cap, which would exclude acetonitrile. There are indeed examples of competition between aryl and acetonitrile coordination in copper(I) complexes.¹⁵ However, in the present case, the aryl moiety is too far for binding to the metal. The differences in the room temperature NMR properties of [Cu(**1**)(CH₃CN)]⁺ and [Cu(**2**)(CH₃CN)]⁺ suggest that these complexes are fluxional, the process being faster for the former. Fluxionality can be observed if the CH₃CN ligand is bound

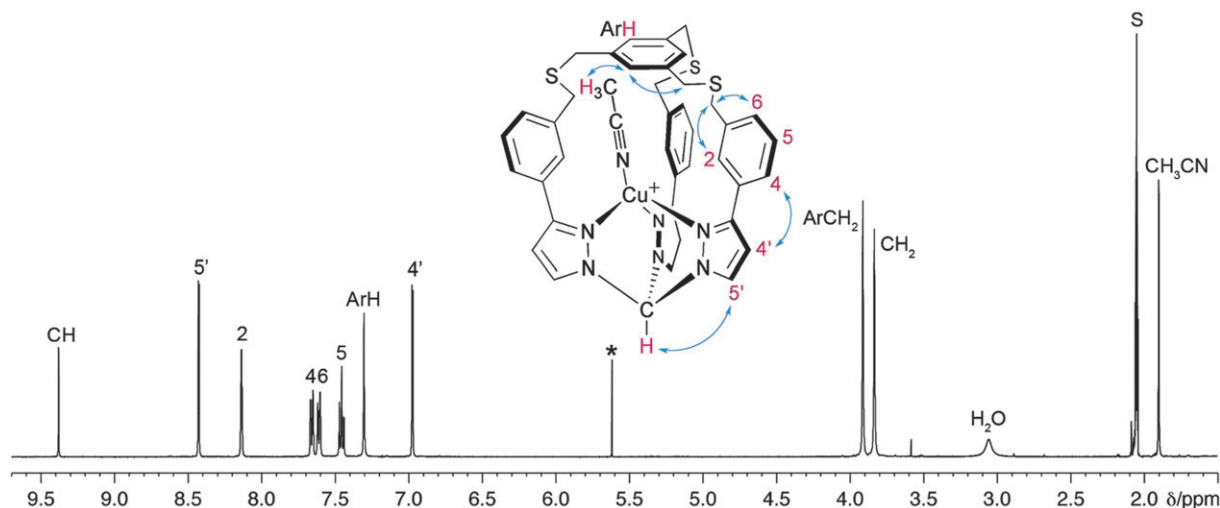


Fig. 2 ¹H NMR spectrum of [Cu(**1**)(CH₃CN)]PF₆ in d₆-acetone at 300 K. The arrows on the structure show NOE correlations.

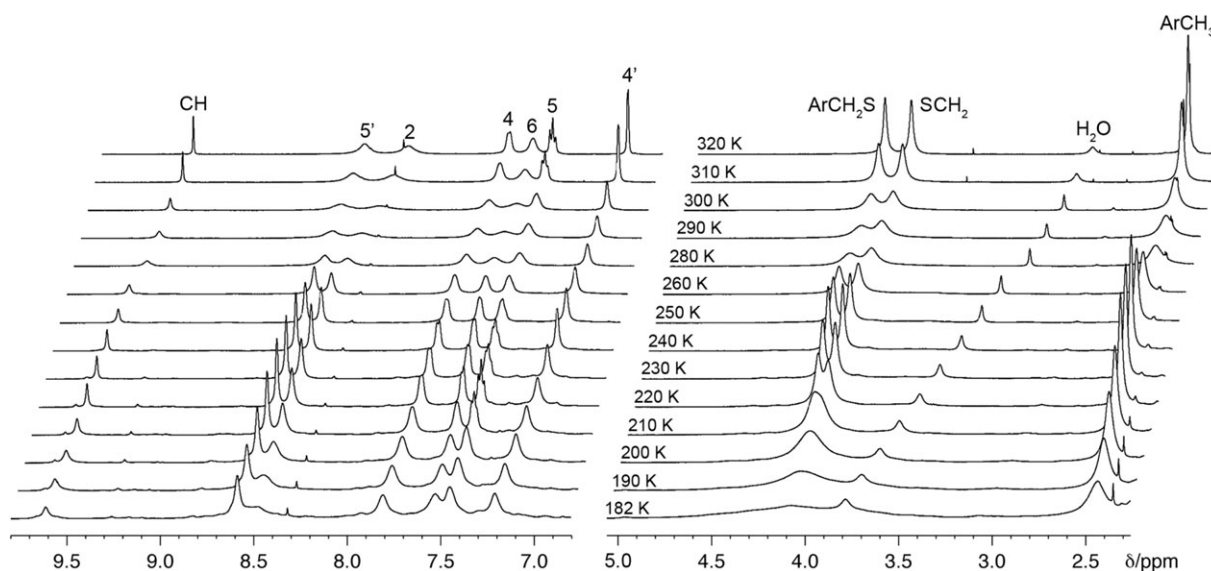
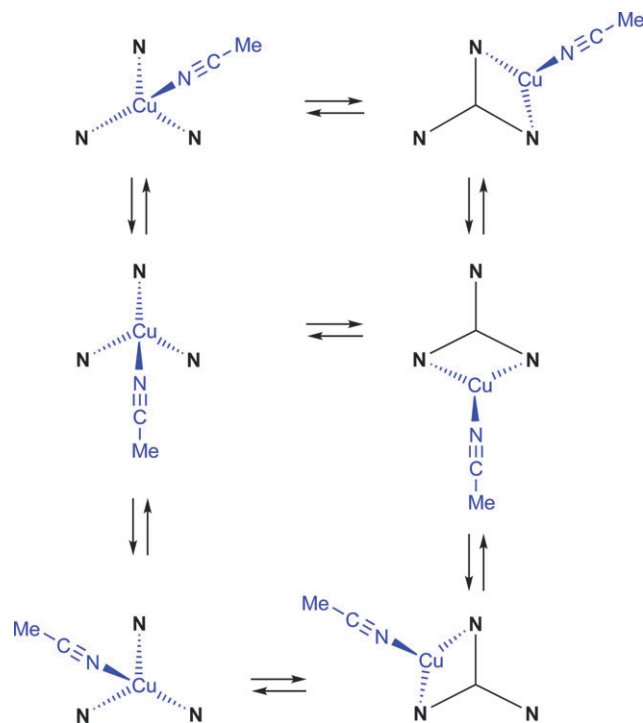


Fig. 3 Variable temperature ^1H NMR spectra of $[\text{Cu}(\mathbf{2})(\text{CH}_3\text{CN})]\text{PF}_6$ in d_6 -acetone.

outside the cavity of the macrobicycles, as represented in the inset of Fig. 2, a hypothesis that is supported by the NOESY experiment. Accommodation of the ancillary ligand within one of the three portals of the macrobicycles is made possible by deformations involving the aryl caps, these being more hindered, and therefore less flexible in **2** by comparison with **1**. The coordination sphere of copper(i) is probably close to a deformed tetrahedron. The resulting complexes having C_{2v} “instantaneous” symmetry, the fluxional processes change it to the observed average C_{3v} symmetry, which involves simultaneous hopping of copper(i) and the bound CH_3CN between the three openings of the macrobicycles (left side of Scheme 3).

This model has however to be refined in order to account for the peculiar low temperature behavior of $[\text{Cu}(\mathbf{2})(\text{CH}_3\text{CN})]^+$. In particular, the relatively well-resolved spectrum obtained at ~ 240 K could be due to a species in which the coordination sphere of copper(i) is trigonal planar. This is, for example, possible if the Cu^+ cation is bound in κ^2 coordination mode to two pyrazole nitrogen atoms of the macrobicycles, leaving the third one uncoordinated, and to the acetonitrile molecule (right side of Scheme 3). The transition between the tetrahedral and trigonal geometries relieves the steric strain associated with the former at the expense of a decrease of the coordination number of the Cu^+ cation. In both coordination modes, decoordination of the ancillary CH_3CN ligand leaves trigonal pyramidal $\text{Cu}(\text{i})$ as transient intermediate.

The bound acetonitrile molecule can be removed to form $[\text{Cu}(\mathbf{1})]^+$ and $[\text{Cu}(\mathbf{2})]^+$. This is accomplished by treatment of $[\text{Cu}(\mathbf{1})(\text{CH}_3\text{CN})]^+$ and $[\text{Cu}(\mathbf{2})(\text{CH}_3\text{CN})]^+$, respectively, with acetone, evaporation of the solvent, and heating the solid residue in vacuum. Noticeably, whereas removal of bound CH_3CN occurs readily at $35\text{--}45$ °C in the case of $[\text{Cu}(\mathbf{2})(\text{CH}_3\text{CN})]^+$, the process has to be repeated several times with heating at 100 °C in the case of $[\text{Cu}(\mathbf{1})(\text{CH}_3\text{CN})]^+$. The ^1H NMR spectra of $[\text{Cu}(\mathbf{1})]^+$ and $[\text{Cu}(\mathbf{2})]^+$ show signals that are broadened and shifted by comparison with those of $[\text{Cu}(\mathbf{1})(\text{CH}_3\text{CN})]^+$ and $[\text{Cu}(\mathbf{2})(\text{CH}_3\text{CN})]^+$ (Table 1). Strongest shifts are experienced by protons 2-H (-0.11 and -0.11 ppm) and CH_2S (-0.10 and



Scheme 3 Dynamic processes occurring in the acetonitrile $\text{Cu}(\text{i})$ complexes of macrobicycles **1** and **2**.

-0.09 ppm) of $[\text{Cu}(\mathbf{1})]^+$ and $[\text{Cu}(\mathbf{2})]^+$, respectively, which are in the vicinity of the bridging sulfur atoms. In addition, the methine proton of **1** experiences a strong upfield shift ($+0.14$ ppm), which is not observed in the case of $[\text{Cu}(\mathbf{2})]^+$ (-0.01 ppm). The $^1\text{H}/^1\text{H}$ NOESY 2D NMR spectrum of $[\text{Cu}(\mathbf{1})]^+$ shows the same correlations ($\text{CH}_3\text{CN}/\text{ArH}$ excepted) as those found in the case of $[\text{Cu}(\mathbf{1})(\text{CH}_3\text{CN})]^+$. Cooling a solution of $[\text{Cu}(\mathbf{1})]^+$ down to 190 K only broadens the signals, as for $[\text{Cu}(\mathbf{1})(\text{CH}_3\text{CN})]^+$ (Fig. S7, ESI ‡). By contrast, the 190 K ^1H NMR spectrum of $[\text{Cu}(\mathbf{2})]^+$ is dramatically different from that of $[\text{Cu}(\mathbf{2})(\text{CH}_3\text{CN})]^+$ (Fig. S8, ESI ‡), as it shows a multitude of relatively sharp signals,

except in the region of the methylene protons (3.2–5.0 ppm). This suggests that $[\text{Cu}(2)]^+$ exists under different, highly unsymmetrical conformations at this temperature. Upon warming up, these signals gradually disappear at the expense of those observed at 298 K. As noted for the VT ^1H NMR spectra of $[\text{Cu}(2)(\text{CH}_3\text{CN})]^+$ transient sharpening of the signals of $[\text{Cu}(2)]^+$ is also observed at intermediate temperature (240 K). All of these observations suggest that CH_3CN coordination in $[\text{Cu}(1)(\text{CH}_3\text{CN})]^+$ and $[\text{Cu}(2)(\text{CH}_3\text{CN})]^+$ is replaced by intramolecular thioether coordination in $[\text{Cu}(1)]^+$ and $[\text{Cu}(2)]^+$, respectively. The resulting species are highly unsymmetrical and strained, especially in the case of $[\text{Cu}(2)]^+$, which accounts for the spectroscopic differences observed. In addition, the dynamic processes that have been identified for the CH_3CN adducts (Scheme 3) certainly operate also in the case of $[\text{Cu}(1)]^+$ and $[\text{Cu}(2)]^+$.

Although all manipulations were done in an oxygen-free atmosphere, the complexes are not air-sensitive in solution, at least for short periods, and samples for MALDI-TOF experiments could be prepared as usual in the open atmosphere. They showed a peak at m/z corresponding to the monocationic copper(i) adduct of the ligand, a property that was reported in earlier studies for [tris(pyrazolyl)methane]copper(i) acetonitrile complexes.¹²

As mentioned, once dried, $[\text{Cu}(1)(\text{CH}_3\text{CN})]\text{PF}_6$ did not show complete solubility in acetone, even less in dichloromethane. Moreover, white precipitates developed from standing, clarified solutions, indicating that a chemical transformation was taking place. Fortunately, good X-ray quality colorless crystals were obtained from a filtered acetone solution of $[\text{Cu}(1)(\text{CH}_3\text{CN})]\text{PF}_6$ that had been left for a few days at room temperature under argon. They belong to the centrosymmetric trigonal (hexagonal axes) space group $R\bar{3}$. Unexpectedly, the crystals are not made from individual complex molecules, but consist of unidimensional coordination polymers assembled from copper(i) and macrobicyclic **1** (Fig. 4). The complex subunits of the coordination polymer are arranged helically with a ternary periodicity, along the (001) direction of the unit cell whose parameter ($|c| = 15.523 \text{ \AA}$) corresponds to the helix pitch, and their mean axis makes a 21.5° angle with the helix axis. Instead of being equally coordinated by all three pyrazole fragments of the cage, a feature which would have placed it inside the cavity, copper(i) is bound to only two of them (average distance: $2.098(3) \text{ \AA}$), and is located outside, in one of the portals of the macrobicyclic (Fig. 5). This allows the metal cation to reach the sulfur atom (distance $\text{Cu}\cdots\text{S}(12a)$: $2.2268(9) \text{ \AA}$) of another metallated macrobicyclic, and the formation of the coordination polymer. The remaining of the tetrahedral coordination sphere of copper(i) is completed by a water molecule (distance $\text{Cu}\cdots\text{O}$: $2.143(2) \text{ \AA}$) that is located roughly in the center of the cage and oriented by $\text{OH}\cdots\text{N}$ and $\text{OH}\cdots\pi$ hydrogen bonding interactions to the uncomplexed pyrazole nitrogen atom (distance $\text{O}\cdots\text{N}(2b)$: $2.942(3) \text{ \AA}$) and to the mesitylene cap (distance $\text{O}\cdots\text{C}(17)$: $4.806(4) \text{ \AA}$). The distance between the oxygen atom and the centroid of the mesitylene cap is 4.747 \AA , slightly longer than that observed for macrobicyclic **1** (4.521 \AA). To our knowledge, coordination of water to soft copper(i) is quite unusual and represents a unique feature of this system. As a matter of fact,

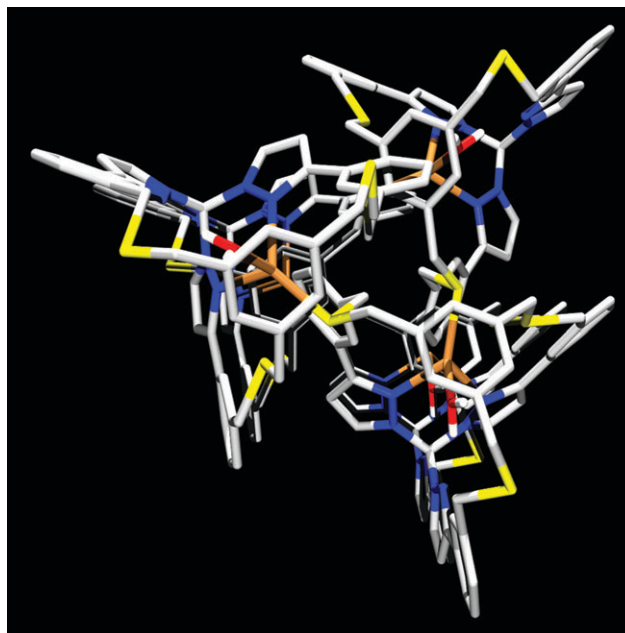


Fig. 4 Ball-and-stick representation of part of the helical coordination polymer in the crystal structure of $[\text{Cu}(1)(\text{H}_2\text{O})]_n(\text{PF}_6)_n$ viewed along the threefold axis of the helix.

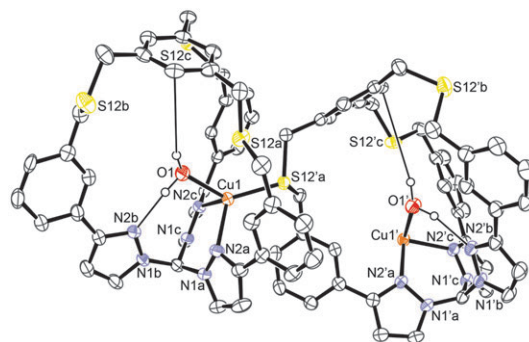


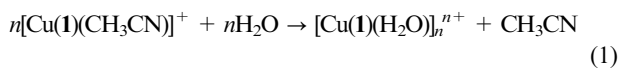
Fig. 5 ORTEP view of two consecutive molecular subunits in the X-ray crystal structure of $[\text{Cu}(1)(\text{H}_2\text{O})]_n(\text{PF}_6)_n$, showing the coordination sphere of Cu(i) and the encapsulated H_2O molecule. Solid lines represent hydrogen bonds. Ellipsoids are drawn at 50% probability level.

rare copper(i)-oxygen bonds have been observed, and it was with carboxylate ligands or in THF adducts.¹⁶ Therefore, the coordination polymer described above can be formulated as $[\text{Cu}(1)(\text{H}_2\text{O})]_n(\text{PF}_6)_n$.

The κ^2 coordination mode of macrobicyclic **1** in the coordination polymer is far from being unprecedented. It is well known that tris(pyrazolyl)methane ligands and their borate analogues can act as simple bidentate chelates, without involving the third arm. Excluding square-planar complexes, this is especially the case for sterically hindered systems, such as $[\text{Cu}\{\text{HB}(3\text{-}(4\text{-}t\text{BuPh})\text{-}5\text{-Mepz})_3\}\text{P}(t\text{Bu})_3]$, in which Cu(i) is tricoordinate,¹⁷ or for metals whose coordination spheres are fulfilled with strong field ligands such as CO or PMe_3 .¹⁸

The following scenario can be proposed for the complexation of copper(i) by macrobicyclic **1** incorporating the tris(pyrazolyl)methane chelate. Reaction with $[\text{Cu}(\text{CH}_3\text{CN})_4]\text{PF}_6$ produces the

soluble complex species $[\text{Cu}(\mathbf{1})(\text{CH}_3\text{CN})]\text{PF}_6$ at first, which then slowly evolves to the insoluble coordination polymer $[\text{Cu}(\mathbf{1})(\text{H}_2\text{O})]_n(\text{PF}_6)_n$. In the latter system two consecutive macrobicyclic ligands bind the bridging metal cation through $\kappa^2\text{-N}(\text{pyrazole})$ and $\kappa^1\text{-S}(\text{thioether})$ coordination, respectively. This places copper(i) slightly outside the cage and allows the metal to satisfy its favored tetrahedral coordination geometry without deformation of the macrobicyclic structure, because there is full room for the fourth ligand (a water molecule) inside the cage. The proposed structure of $[\text{Cu}(\mathbf{1})(\text{CH}_3\text{CN})]\text{PF}_6$ (Fig. 2) differs from that of the monomer complex described above by the following features: (i) acetonitrile ligation, which is replaced by thioether coordination in the polymer, and (ii) probable direct, weak interaction of copper(i) with the pyrazole nitrogen atom that is involved in hydrogen bonding with a water molecule in the polymer. Ketones being known to catalyze substitution reactions in coordination chemistry,¹⁹ and copper(i) being thiophilic, crystallization of the coordination polymer $[\text{Cu}(\mathbf{1})(\text{H}_2\text{O})]_n(\text{PF}_6)_n$ from $[\text{Cu}(\mathbf{1})(\text{CH}_3\text{CN})]\text{PF}_6$ in acetone is not unrealistic. The inclusion of a water molecule, which bridges the metal cation and a pyrazole nitrogen atom *via* hydrogen bonding, could endow the copper(i) complex fragment in the former with increased stability as compared to the latter. As shown in eqn (1), conversion of $[\text{Cu}(\mathbf{1})(\text{CH}_3\text{CN})]^+$ into $[\text{Cu}(\mathbf{1})(\text{H}_2\text{O})]_n^{n+}$ involves release of CH_3CN with concomitant capture of water from the solvent. Comparison of the ^1H NMR spectra of a freshly prepared solution of $[\text{Cu}(\mathbf{1})(\text{CH}_3\text{CN})]^+$ with that of the solution left after deposition of the solid material[¶] shows that the broad singlet of residual H_2O at 3.17 ppm in the former has vanished in the latter. On the contrary, the sharp singlet of CH_3CN at 1.90 ppm is left unchanged, which confirms that bound and free acetonitrile molecules are in exchange at the NMR timescale.



It is also interesting to note that, in spite of the fact that H_2O could fit as axial ligand in the surrounding macrotricyclic cavity, whereas CH_3CN would not, $[\text{Cu}(\mathbf{1})(\text{CH}_3\text{CN})]^+$ is formed rather than the C_{3v} -symmetric $[\text{Cu}(\mathbf{1})(\text{H}_2\text{O})]^+$. This happens at the expense of deformations of the macrobicyclic and distortion of the coordination sphere of the metal cation.

In the scenario detailed above the formation of the coordination polymer is driven by its low solubility. Alternatively, the complexation of copper(i) by macrobicyclic **1** could be analyzed in terms of kinetic and thermodynamic control, the kinetic product being the soluble $[\text{Cu}(\mathbf{1})(\text{CH}_3\text{CN})]\text{PF}_6$ complex, and the thermodynamic product being the insoluble coordination polymer $[\text{Cu}(\mathbf{1})(\text{H}_2\text{O})]_n(\text{PF}_6)_n$. As noted previously, $[\text{Cu}(\mathbf{2})(\text{CH}_3\text{CN})]\text{PF}_6$ gave longstanding clear solutions in d_6 -acetone, a feature which would indicate increased stability of the latter with respect to $[\text{Cu}(\mathbf{1})(\text{CH}_3\text{CN})]\text{PF}_6$.

Summary and conclusion

Two macrobicycles (**1** and **2**) incorporating the tris(pyrazolyl)methane scorpionate ligand and closed by aryl caps have been

[¶] Wet acetone was employed, as checked by ^1H NMR prior to complexation studies.

synthesized from acyclic tris(pyrazolyl)methane precursors bearing appropriate functions. The X-ray crystal structure of the prototypical member of this family of macrobicycles (**1**) showed that the tris(pyrazolyl)methane ligand fragment is highly preorganized for coordination to metal cations favoring tetrahedral geometries, while the surrounding cavity provides only limited space for an ancillary ligand. Acetone solutions obtained after combination of **1** and $[\text{Cu}(\text{CH}_3\text{CN})_4]\text{PF}_6$ evolved to a crystalline material that could be analyzed by X-ray crystallography. The crystals contain helical arrangements of copper-bridged macrobicycles, which form coordination polymers. Unexpectedly, instead of sitting inside the cages the copper(i) cations link two adjacent molecules by coordination to two pyrazole nitrogens and one thioether sulfur. Their coordination sphere is completed by a water molecule that resides inside the cage and is hydrogen bonded to the remaining, free pyrazole nitrogen. Therefore the coordination polymers can be formulated as $[\text{Cu}(\mathbf{1})(\text{H}_2\text{O})]_n(\text{PF}_6)_n$. Comparison of the ^1H NMR properties of the soluble adducts of macrobicycles **1** and **2** with copper(i) suggests that these are fluxional complexes, which are direct precursors of the coordination polymers by ligand substitution: in acetone, the acetonitrile complex $[\text{Cu}(\mathbf{1})(\text{CH}_3\text{CN})]^+$ is slowly converted into the insoluble coordination polymer $[\text{Cu}(\mathbf{1})(\text{H}_2\text{O})]_n^{n+}$.

Water complexation and activation in transition metal complexes featuring hydrogen bonding sites that are not involved in metal coordination have been described.²⁰ However the prototypical tris(pyrazolyl)methane-incorporating macrobicyclic **1** has the rare and interesting ability to bind simultaneously with the same type of donor atoms (pyrazole nitrogen) a metal cation (coordination bond $\text{N}-\text{Cu}^+$) and a water molecule (hydrogen bond $\text{N}\cdots\text{H}(\text{O})$). This result is an illustration of a possible consequence of squeezing the coordination environment of a metal.

As the stability in solution of the copper(i) complexes of macrobicyclic **2** is increased as compared to those of **1**, further work will study the reactivity of $[\text{Cu}(\mathbf{2})(\text{CH}_3\text{CN})]^+$ and $[\text{Cu}(\mathbf{2})]^+$ with small anionic ligands and investigate the possibility of these complexes to mimic active sites of metalloproteins, such as nitrite reductase.²¹

Experimental

General

1,3,5-Tribromomethylbenzene (**4**),²² 1,3,5-tribromomethyl-2,4,6-trimethylbenzene (**5**),²³ and $[\text{Cu}(\text{CH}_3\text{CN})_4](\text{PF}_6)_4$ ²⁴ were prepared according to the literature. Unless otherwise stated all reactions were performed under argon using standard Schlenk techniques. Dimethylformamide was filtered on alumina and stored over 3 Å molecular sieves. Silica for column chromatography was from Merck (Kieselgel 60). NMR spectra were obtained using Bruker Avance 300 and DRX 500 spectrometers. Mass spectra were obtained with a Bruker Daltonix Proflex III spectrometer (MALDI-TOF, dithranol matrix). Melting points were measured with a Büchi Melting Point B-545 apparatus and are uncorrected. Elemental analyses were run with an EA1108 CHNS Fisons Instrument analyser.

Synthesis

Macrobicycle 1. A solution of **3** (0.210 g, 0.360 mmol) and 1,3,5-tribromomethylbenzene **4** (0.129 g, 0.360 mmol) in DMF (150 cm³) was added dropwise to a stirred suspension of K₂CO₃ (0.300 g, 2.16 mmol) in DMF (300 cm³) at 55 °C over 4 days. After 24 h stirring the solvent was removed *in vacuo* and the residue partitioned between CH₂Cl₂ and water. The organic layer was washed with brine and dried over MgSO₄. Purification of the crude product by chromatography (silica 70–230 mesh, CH₂Cl₂) followed by crystallization from CH₂Cl₂–heptane afforded 0.070 g of **1** as colorless crystals. Yield: 28%. mp > 300 °C (dec). Found: C, 68.21; H, 5.12; N, 11.71; S, 12.92. Calc. for C₄₀H₃₄N₆S₃·0.5 H₂O: C, 68.26; H, 5.02; N, 11.95; S, 13.64%. δ_{H} (500 MHz, CDCl₃; Me₄Si) 8.13 (1 H, br s, CH), 7.66 (3 H, s, 2-H), 7.66 (3 H, d, ²J 2.5, 5'-H), 7.42 (3 H, d, ²J 7.6, 4-H), 7.38 (3 H, d, ²J 7.6, 6-H), 7.31 (3 H, t, ²J 7.6, 5-H), 7.03 (3 H, s, ArH), 6.63 (3 H, d, ²J 2.5, 4'-H), 3.62 (6 H, s, CH₂), 3.60 (6 H, s, CH₂). δ_{H} (500 MHz, CD₂Cl₂; Me₄Si) 8.16 (1 H, s, CH), 7.73 (3 H, d, ³J 2.5, 5'-H), 7.68 (3 H, t, ⁴J 1.5, 2-H), 7.45 (3 H, ddd, ³J 7.5 Hz, ⁴J 1.5, 4-H), 7.42 (3 H, ddd, ³J 7.5, ⁴J 1.5, 6-H), 7.34 (3 H, t, ³J 7.5, 5-H), 7.08 (3 H, s, ArH), 6.67 (3 H, d, ³J 2.5, 4'-H), 3.67 (6 H, s, ArCH₂S), 3.63 (6 H, s, CH₂S). δ_{H} (500 MHz, d₆-acetone; Me₄Si) 9.02 (1 H, s, CH), 8.04 (3 H, d, ³J 2.5, 5'-H), 7.96 (3 H, br s, 2-H), 7.51 (3 H, br d, ³J 7.7, 4-H), 7.43 (3 H, br d, ³J 7.7, 6-H), 7.32 (3 H, t, ³J 7.7, 5-H), 7.23 (3 H, s, ArH), 6.70 (3 H, d, ³J 2.5, 4'-H), 3.81 (6 H, s, ArCH₂S), 3.73 (6 H, s, CH₂S). δ_{C} (75 MHz, CDCl₃; Me₄Si) 152.7, 138.9, 138.1, 133.5, 130.9 (5'-C), 129.0 (5-C), 128.6 (6-C), 128.4 (Ar-C), 127.4 (2-C), 124.8 (4-C), 105.1 (4'-C), 81.9 (CH), 36.4 (CS) 36.3 (CS); δ_{C} (125 MHz, CD₂Cl₂; Me₄Si) 152.8 (3'-C), 139.3 (ArC-C), 138.4 (1-C), 135.6 (3-C), 131.1 (5'-C), 129.0 (5-C), 128.9 (6-C), 128.3 (ArH-C), 127.4 (2-C), 124.9 (4-C), 105.1 (4'-C), 81.8 (CH), 36.7 (ArCH₂S), 36.4 (CH₂S). δ_{C} (125 MHz, d₆-acetone; Me₄Si) 152.7, 140.4, 138.6, 134.8, 132.4, 129.5, 129.5, 128.7, 127.6, 125.4, 104.5, 81.1, 37.6, 37.1. *m/z* (MALDI-TOF) 694.87 (M⁺).

Macrobicycle 2. A solution of **3** (0.200 g, 0.344 mmol) and 1,3,5-tribromomethyl-2,4,6-trimethylbenzene **5** (0.142 g, 0.356 mmol) in DMF (50 cm³) was added dropwise to a stirred suspension of K₂CO₃ (0.296 g, 2.142 mmol) in DMF (150 cm³) at 60 °C over 8 h. After overnight stirring the solvent was removed *in vacuo*. Purification of the crude product by flash column chromatography (silica 230–400 mesh, 2% AcOEt in CH₂Cl₂) afforded **2** (0.090 g) as a colorless solid. Yield: 32%. mp 272 °C (dec). Found: C, 68.57; H, 5.76; N, 10.94; S 11.96. Calc'd for C₄₃H₄₀N₆S₃·H₂O: C, 68.40; H, 5.60; N, 11.13; S, 12.74%. δ_{H} (500 MHz, CDCl₃; Me₄Si) 8.17 (1 H, s, CH), 7.73 (3 H, d, ³J 2.5, 5'-H), 7.58 (3 H, br s, 2-H), 7.43 (3 H, ddd, ³J 7.5, ⁴J 1.5, 4-H), 7.32 (3 H, ddd, ³J 7.5, ⁴J 1.5, 6-H), 7.29 (3 H, t, ³J 7.5, 5-H), 6.64 (3 H, d, ³J 2.5, 4'-H), 3.73 (6 H, s, CH₂), 3.52 (6 H, s, CH₂), 2.04 (3 H, s, CH₃). δ_{H} (500 MHz, CD₂Cl₂; Me₄Si) 8.23 (1 H, s, CH), 7.78 (3 H, d, ³J 2.5, 5'-H), 7.52 (3 H, br s, 2-H), 7.60 (3 H, ddd, ³J 7.5, ⁴J 1.6, 4-H), 7.36 (3 H, ddd, ³J 7.5, 6-H), 7.31 (3 H, t, ³J 7.5, 5-H), 6.71 (3 H, d, ³J 2.5, 4'-H), 3.73 (6 H, s, ArCH₂S), 3.50 (6 H, s, CH₂S), 2.01 (3 H, s, CH₃). δ_{C} (125 MHz, CD₂Cl₂; Me₄Si) 152.6, 139.8,

136.8, 133.7, 131.6, 129.3, 128.7, 127.3, 124.9, 105.5, 31.7, 16.7 (3 missing signals). *m/z* (MALDI-TOF) 738.02 (M + H⁺).

[Cu(1)(CH₃CN)]PF₆. A solution of [Cu(CH₃CN)₄]PF₆ (0.012 g, 0.0295 mmol) in CH₃CN (2 cm³) was added to a solution of **1** (0.0210 g, 0.0302 mmol) in CH₂Cl₂ (3 cm³). After 3 h stirring, the solvents were removed *in vacuo* leaving a colorless residue which was dried overnight at 35 °C. δ_{H} (500 MHz, CD₃CN; Me₄Si) 8.59 (1 H, s, CH), 8.01 (3 H, d, ³J 2.6, 5'-H), 7.91 (3 H, br s, 2-H), 7.51 (3 H, ddd, ³J 7.7, ⁴J 1.5, 4-H), 7.47 (3 H, ddd, ³J 7.7, ⁴J 1.5, 6-H), 7.36 (3 H, t, ³J 7.7, 5-H), 7.13 (3 H, s, ArH), 6.73 (3 H, d, ³J 2.6, 4'-H), 3.74 (12 H, s, CH₂). δ_{H} (600 MHz, d₆-acetone; Me₄Si) 9.41 (1 H, s, CH), 8.44 (3 H, d, ³J 3.0, 5'-H), 8.14 (3 H, br s, 2-H), 7.67 (3 H, dt, ³J 7.8, 4-H), 7.62 (3 H, dt, ³J 7.8, 6-H), 7.46 (3 H, t, ³J 7.8, 5-H), 7.32 (3 H, s, ArH), 6.99 (3 H, d, ³J 3.0 Hz, 4'-H), 3.92 (6 H, s, ArCH₂S), 3.85 (6 H, s, CH₂S), 1.90 (3 H, s, CH₃CN). δ_{H} (500 MHz, CD₂Cl₂; Me₄Si) 8.82 (1 H, s, CH), 8.24 (3 H, d, ³J 2.7, 5'-H), 8.05 (3 H, br s, 2-H), 7.61 (3 H, d, ³J 7.6, 4-H), 7.51 (3 H, d, ³J 7.6 Hz, 6-H), 7.43 (3 H, t, ³J 7.6, 5-H), 7.19 (3 H, s, ArH), 6.69 (3 H, d, ³J 2.7, 4'-H), 3.83 (6 H, s, ArCH₂S), 3.79 (6 H, s, CH₂S), 1.66 (3 H, s, CH₃CN). δ_{C} (125 MHz, d₆-acetone; Me₄Si) 154.6, 139.7, 138.7, 135.3, 131.5, 130.8, 130.2, 128.9, 127.3, 127.2, 106.2, 78.7, 55.0, 37.0, 36.2, 3.7. *m/z* (MALDI-TOF) 756.82 (Cu(1)–CH₃CN–PF₆)⁺.

[Cu(1)(H₂O)]·PF₆·1/3C₃H₆O·1/9H₂O. [Cu(1)(CH₃CN)]PF₆ was dissolved in d₆-acetone, leaving a colorless residue that was discarded. The filtrate was placed in an NMR tube and stored at room temperature. Needle-like crystals suitable for X-ray diffraction appeared after 5 days.

[Cu(2)(CH₃CN)]PF₆. A solution of [Cu(CH₃CN)₄]PF₆ (0.0110 g, 0.0295 mmol) in CH₃CN (2 cm³) was added to a suspension of **2** (0.0218 g, 0.0296 mmol) in CH₂Cl₂ (4 cm³). After 3 h stirring, the solvents were removed *in vacuo* leaving a colorless residue, which was dried overnight at 35 °C. δ_{H} (500 MHz, d₆-acetone, 298 K; Me₄Si) 9.40 (1 H, s, CH), 8.45 (3 H, br s, 5'-H), 8.17 (3 H, br s, 2-H), 7.63 (3 H, br s, 4-H), 7.50 (3 H, br s, 6-H), 7.39 (3 H, br s, 5-H), 7.01 (3 H, s, 4'-H), 4.09 (6 H, br s, ArCH₂S), 3.91 (6 H, br s, CH₂), 2.45 (9 H, br s, CH₃), 2.03 (3 H, s, CH₃CN). *m/z* (MALDI-TOF) 798.08 (Cu(2)–CH₃CN–PF₆)⁺.

[Cu(1)]PF₆. Mixing [Cu(CH₃CN)₄]PF₆ (0.00270 g, 7.22 × 10⁻⁶ mol) and **1** (0.00502 g, 7.22 × 10⁻⁶ mol) in d₆-acetone produced a solution, which was evaporated *in vacuo*. Further drying at 45 °C for 22 h afforded [Cu(1)(CH₃CN)]PF₆ (¹H NMR in d₆-acetone). The same procedure was repeated three times at 100 °C to leave [Cu(1)]PF₆ along with insoluble matter. δ_{H} (500 MHz, d₆-acetone, 298 K; Me₄Si) 9.55 (1 H, s, CH), 8.46 (3 H, s, 5'-H), 8.03 (3 H, s, 2-H), 7.62 (3 H, d, ³J 7.5, 4-H), 7.57 (3 H, d, ³J 7.5, 6-H), 7.43 (3 H, t, ³J 7.5, 5-H), 7.29 (3 H, s, ArH), 6.97 (3 H, d, ³J 2.5, 4'-H), 3.90 (6 H, s, ArCH₂S), 3.75 (6 H, s, CH₂).

[Cu(2)]PF₆. Mixing [Cu(CH₃CN)₄]PF₆ (0.00255 g, 6.84 × 10⁻⁶ mol) and **1** (0.00495 g, 6.72 × 10⁻⁶ mol) in d₆-acetone produced a solution, which was evaporated *in vacuo*. Further drying at 35 °C for 18 h afforded [Cu(2)(CH₃CN)]PF₆ (¹H NMR in d₆-acetone). The same procedure was repeated

once at 35 °C overnight to leave [Cu(2)]PF₆ quantitatively. δ_{H} (500 MHz, d₆-acetone, 298 K; Me₄Si) 9.39 (1 H, br s, CH), 8.45 (3 H, br s, 5'-H), 8.06 (3 H, s, 2-H), 7.60 (3 H, br s, 4-H), 7.45 (3 H, br s, 6-H), 7.35 (3 H, br s, 5-H), 6.98 (3 H, br s, 4'-H), 4.07 (6 H, br s, ArCH₂S), 3.82 (6 H, br s, CH₂), 2.42 (9 H, br s, CH₃).

X-Ray crystallography

Colorless single-crystal specimens of prismatic shapes of 21·1.5H₂O·0.5CH₂Cl₂·0.5C₂H₆O and [Cu(1)(H₂O)]·PF₆·1/3C₃H₆O·1/9H₂O were selected for the X-ray diffraction experiments at $T = 110(2)$ and $115(2)$ K, respectively. They were mounted with silicon grease on the tips of glass capillaries. Diffraction data were collected on a Nonius KappaCCD diffractometer²⁵ equipped with a nitrogen jet stream low-temperature system (Oxford Cryosystems). The X-ray source was graphite-monochromated Mo-K α radiation ($\mu = 0.71073$ Å) from a sealed tube. In both cases, lattice parameters were obtained by a least-squares fit to the optimized setting angles of the collected reflections. Intensity data were recorded as φ - and ω -scans with κ offsets. No significant intensity decay or temperature drift was observed during the data collections. Data were reduced by using DENZO software²⁶ without applying absorption corrections, the missing absorption corrections being partially compensated by the data scaling procedure in the data reduction. The structures were solved by direct methods using the SIR97 program.²⁷ Refinements were carried out by full-matrix least-squares on F^2 using the SHELXL97 program²⁸ and the complete set of reflections. Anisotropic thermal parameters were used for non-hydrogen atoms. In both crystal structure determinations, most of the hydrogen atoms were located in the Fourier synthesis. They were placed at calculated positions using a riding model, except one of the water molecule encapsulated by **1** and those of the water molecule in the coordination sphere of the metal center, which were, respectively, constrained and restrained to the mean Ow–H bond distance (~ 0.98 Å) observed from neutron experiments.²⁹ The isotropic thermal factors of all hydrogen atoms were fixed at 1.3 times the equivalent isotropic displacement parameter of the corresponding bonded atom. The hydrogen atoms of a water molecule with a site occupation factor of 1/9 in the copper complex crystal structure, and another one of the disordered water molecule encapsulated by **1**, were not found.

Compound 21·1.5H₂O·0.5CH₂Cl₂·0.5C₂H₆O crystallizes in the triclinic system (space group $P\bar{1}$). The asymmetric unit consists of two non-equivalent macrobicycles **1**, one non-disordered and one disordered, as well as co-crystallized water, dichloromethane and ethanol solvent molecules. The disorder of the macrobicycle is observed over two close positions (site occupation factors 0.5/0.5) and involves one of the three *m*-phenylene spacers and the benzene cap. This macrobicycle encapsulates a disordered water molecule over two positions, one inside and one outside **1**, exhibiting site occupation factors of 0.5/0.5. The dichloromethane molecule was found close to the disordered macrobicycle, sharing its occupied region with a couple of ethanol and water molecules. These CH₂Cl₂, H₂O and C₂H₆O molecules were refined with site occupation

factors of 0.5. The two highest residuals (1.54 and 1.06 e Å⁻³) appear as a partial unachieved modelling of the disorder close to the position of two sulphur atoms. In order to drive the refinement towards a meaningful model, 383 restraints were used. They were applied to all disordered parts of the molecular structure and concern bonding distances (DFIX instruction), flatness of phenyl rings (FLAT instruction), rigid bond and isotropic restraints on the anisotropic displacement parameters (DELU and ISOR instructions).

Compound [Cu(1)(H₂O)]·PF₆·1/3C₃H₆O·1/9H₂O crystallizes in the trigonal system (space group $R\bar{3}$, hexagonal axes). The asymmetric unit consists of one copper complex [Cu(1)]⁺, one counter-ion PF₆⁻ and co-crystallized water and acetone molecules. One water molecule is found in the coordination sphere of the metal center, which is tetrahedral. Two remaining C₃H₆O and H₂O solvent molecules were refined with site occupation factors of 1/3 and 1/9, the acetone being disordered around a threefold inversion axis at (0, 0, 0) and the water molecule occupying a special position on this axis at (0, 0, z). The refinement of the water molecule with this low site occupation factor (1/3 lower than the site symmetry) was based on the residual initially observed at the oxygen atom position (1.83 e Å⁻³) and on the refinement of its anisotropic displacement parameters. In addition, even if higher residuals (not necessarily corresponding to any atom) are expected on special positions, the presence of a solvent molecule is also presumed based on large accessible regions in the unit cell. Indeed, even after determination of the crystal structure, voids of 217 Å³ are observed close to the regions occupied by this water molecule. A careful examination of the residual density seems to indicate no further molecules. However, the consideration of another disordered solvent molecule instead of water cannot be completely excluded due to the presence of several diffuse residuals in the same region (the two highest residuals, 0.90 and 0.69 e Å⁻³, were found out of the threefold inversion axis at 1.11 and 2.30 Å from the oxygen atom of this water molecule). The *m*-phenylene spacers of two arms of the macrobicycle were found partially disordered (each one over two close positions) and they were refined with sites occupation factors of 0.6/0.4 and 0.7/0.3. In order to drive the refinement towards a meaningful model, 201 restraints were used. They were applied to all disordered parts of the molecular structure and concern bonding distances (DFIX instruction), flatness of phenyl rings (FLAT instruction), rigid bond and isotropic restraints on the anisotropic displacement parameters (DELU and ISOR instructions).

Relevant experimental crystal data and refinement details are summarized in Table S2 (ESI†). Crystallographic views were generated using ORTEP III for windows.³⁰

References

- 1 K. Maruoka, A. B. Conception, N. Hirayama and H. Yamamoto, *J. Am. Chem. Soc.*, 1990, **112**, 7422–7423; M. Ray, G. P. A. Yap, A. L. Rheingold and A. S. Borovik, *J. Chem. Soc., Chem. Commun.*, 1995, 1777–1778; M. H. Chisholm and N. W. Eilerts, *Chem. Commun.*, 1996, 853–854; M. Ray, B. S. Hammes, G. P. A. Yap, A. L. Rheingold and A. S. Borovik, *Inorg. Chem.*, 1998, **37**, 1527–1532; J. R. Hagadorn, L. Que, Jr. and W. B. Tolman, *J. Am. Chem. Soc.*, 1998, **120**, 13531–13532; X. Hu, I. Castro-Rodriguez and K. Meyer, *Chem. Commun.*, 2004, 2164–2165;

- I. Nieto, F. Cervantes-Lee and J. M. Smith, *Chem. Commun.*, 2005, 3811–3813; C. Zimmermann, F. W. Heinemann and A. Grohmann, *Eur. J. Inorg. Chem.*, 2005, 3506–3512; U. Lünig and F. Fahrenkrug, *Eur. J. Org. Chem.*, 2006, 916–923.
- 2 R. R. Schrock, *Acc. Chem. Res.*, 2005, **38**, 955–962; P. L. Holland, *Can. J. Chem.*, 2005, **83**, 296–301.
 - 3 Early examples: J. P. Collman, R. R. Gagne, C. A. Reed, T. R. Halbert, G. Lang and W. T. Robinson, *J. Am. Chem. Soc.*, 1974, **97**, 1427–1439; A. R. Battersby, D. G. Buckley, S. G. Hartley and M. D. Turnbull, *J. Chem. Soc., Chem. Commun.*, 1976, 879–881; J. E. Baldwin, T. Klose and M. Peters, *J. Chem. Soc., Chem. Commun.*, 1976, 881–883; M. Momenteau, B. Look, J. Mispelter and E. Bisagni, *Nouv. J. Chim.*, 1979, **3**, 77–79.
 - 4 D. H. Camacho, E. V. Salo, J. W. Ziller and Z. Guan, *Angew. Chem., Int. Ed.*, 2004, **43**, 1821–1825.
 - 5 K. Maruszewski, D. P. Strommen and J. R. Kincaid, *J. Am. Chem. Soc.*, 1993, **115**, 8345–8350.
 - 6 M. Yoshizawa and M. Fujita, *Pure Appl. Chem.*, 2005, **77**, 1107–1112; J. Rebek Jr, *Angew. Chem., Int. Ed.*, 2005, **44**, 2068–2078; D. Fiedler, D. H. Leung, R. G. Bergman and K. N. Raymond, *Acc. Chem. Res.*, 2005, **38**, 349–358.
 - 7 S. Trofimenko, *Chem. Rev.*, 1993, **93**, 943–980.
 - 8 N. Kitajima, K. Fujisawa and Y. Moro-oka, *J. Am. Chem. Soc.*, 1990, **112**, 3210–3212; N. Kitajima, K. Fujisawa, M. Tanaka and Y. Moro-oka, *J. Am. Chem. Soc.*, 1992, **114**, 9232–9233; D. Qiu, L. Kilpatrick, N. Kitajima and T. G. Spiro, *J. Am. Chem. Soc.*, 1994, **116**, 2585–2590.
 - 9 R. Alsfasser, S. Trofimenko, A. Looney, G. Parkin and H. Vahrenkamp, *Inorg. Chem.*, 1991, **30**, 4098–4100; A. Looney, G. Parkin, R. Alsfasser, M. Ruf and H. Vahrenkamp, *Angew. Chem., Int. Ed. Engl.*, 1992, **31**, 92–93; R. Alsfasser, M. Ruf, S. Trofimenko and H. Vahrenkamp, *Chem. Ber.*, 1993, **126**, 703–710; A. Looney, R. Han, K. McNeill and G. Parkin, *J. Am. Chem. Soc.*, 1993, **115**, 4690–4697.
 - 10 M. C. Keyes, B. M. Chamberlain, S. A. Caltagirone, J. A. Halfen and W. B. Tolman, *Organometallics*, 1998, **17**, 1984–1992.
 - 11 D. L. Reger, J. E. Collins, A. L. Rheingold, L. M. Liable-Sands and G. P. A. Yap, *Organometallics*, 1997, **16**, 349–353.
 - 12 D. L. Reger, J. E. Collins, A. L. Rheingold and L. M. Liable-Sands, *Organometallics*, 1996, **15**, 2029–2032.
 - 13 L. Wang and J.-C. Chambron, *Org. Lett.*, 2004, **6**, 747–750.
 - 14 A. H. Lewin, R. J. Michl, P. Ganis and U. Lepore, *J. Chem. Soc., Chem. Commun.*, 1972, 661–662; P. Roussel and P. Scott, *J. Am. Chem. Soc.*, 1998, **120**, 1070–1071; B. A. Jazdzewski, V. G. Young, Jr. and W. B. Tolman, *Chem. Commun.*, 1998, 2521–2522; P. L. Holland and W. B. Tolman, *J. Am. Chem. Soc.*, 2000, **122**, 6331–6332; S. Yokota, Y. Tachi, N. Nishiwaki, M. Ariga and S. Itoh, *Inorg. Chem.*, 2001, **40**, 5316–5317; F.-B. Xu, Q.-S. Li, L.-Z. Wu, X.-B. Leng, Z.-C. Li, X.-S. Zeng, Y. L. Chow and Z.-Z. Zhang, *Organometallics*, 2003, **22**, 633–640; B. A. Gandhi, O. Green and J. N. Burstyn, *Inorg. Chem.*, 2007, **46**, 3816–3825.
 - 15 T. Osako, Y. Ueno, Y. Tachi and S. Itoh, *Inorg. Chem.*, 2003, **42**, 8087–8097.
 - 16 J. R. Hagadorn, T. I. Zahn, L. Que, Jr and W. B. Tolman, *J. Chem. Soc., Dalton Trans.*, 2003, 1790–1794.
 - 17 R. R. Conry, G. Ji and A. A. Tipton, *Inorg. Chem.*, 1999, **38**, 906–913.
 - 18 A. Macchioni, G. Bellachioma, G. Cardaci, V. Gramlich, H. Rügger, S. Terenzi and L. M. Venanzi, *Organometallics*, 1997, **16**, 2139–2145.
 - 19 E. Engeldinger, D. Armspach, D. Matt and P. G. Jones, *Chem.–Eur. J.*, 2003, **9**, 3091–3105.
 - 20 J. C. Mareque-Rivas, R. Prabaharan and R. Torres Martín de Rosales, *Chem. Commun.*, 2004, 76–77.
 - 21 M. Kukimoto, M. Nishiyama, M. E. P. Murphy, S. Turley, E. T. Adman, S. Horinouchi and T. Beppu, *Biochemistry*, 1994, **33**, 5246–5252; H. J. Wijma, L. J. C. Jeuken, M. P. Verbeet, F. A. Armstrong and G. W. Canters, *J. Biol. Chem.*, 2006, **281**, 16340–16346 and references therein.
 - 22 E. Díez-Barra, J. C. García-Martínez, S. Merino, R. del Rey, J. Rodríguez-López, P. Sánchez-Verdú and J. Tejada, *J. Org. Chem.*, 2001, **66**, 5664–5670.
 - 23 S. K. Armstrong, S. Clunas and K. W. Muir, *Synthesis*, 1999, 993–998.
 - 24 G. J. Kubas, *Inorg. Syntheses*, 1990, **28**, 90–92.
 - 25 B. Nonius, in *COLLECT, Data Collection Software*, BV Nonius, Delft, The Netherlands, 1998.
 - 26 Z. Otwinowski and W. Minor, *Methods Enzymol.*, 1997, **276**, 306–326.
 - 27 A. Altomare, M. C. Burla, M. Camalli, G. L. Cascarano, C. Giacovazzo, A. Guagliardi, A. G. G. Moliterni, G. Polidori and R. Spagna, *J. Appl. Crystallogr.*, 1999, **32**, 115–119.
 - 28 G. M. Sheldrick, in *SHELXS-97, Program for the Solution of Crystal Structures*, University of Göttingen, Göttingen, Germany, 1997.
 - 29 E. Espinosa, C. Lecomte, E. Molins, S. Veintemillas, A. Cousson and W. Paulus, *Acta Crystallogr., Sect. B*, 1996, **52**, 519–534; I. Mata, E. Espinosa, E. Molins, S. Veintemillas, W. Maniukiewicz, C. Lecomte, A. Cousson and W. Paulus, *Acta Crystallogr., Sect. A*, 2006, **62**, 365–378.
 - 30 L. J. Farrugia, *J. Appl. Crystallogr.*, 1999, **32**, 837–838.